Caltrans 3477 Practical Performance Indices for Signalized Corridors

Final Report

PI: Ketan Savla, ksavla@usc.edu

(co-authors: Xinyi Wu, Zhexian Li, Zixiong Wang)

TECHNICAL REPORT DOCUMENTATION PAGE

1. Report No. PSR 23-07	**2. Government Accession No.** N/A	**3. Recipient's Catalog No.** N/A
4. Title and Subtitle Practical Performance Indices for Signalized Corridors		**5. Report Date** December 31, 2024 **6. Performing Organization Code** N/A
7. Author(s) Ketan Savla https://orcid.org/0000-0002-1668-6380		**8. Performing Organization Report No.** PSR 23-07 TO 077
9. Performing Organization Name and Address METRANS Transportation Consortium University of Southern California University Park Campus, RGL 216 Los Angeles, CA 90089-0626		**10. Work Unit No.** N/A **11. Contract or Grant No.** USDOT Grant 69A3551747109 [Caltrans TO 071]
12. Sponsoring Agency Name and Address U.S. Department of Transportation Office of the Assistant Secretary for Research and Technology 1200 New Jersey Avenue, SE, Washington, DC 20590		**13. Type of Report and Period Covered** Final report (March 2024 – December 2024 **14. Sponsoring Agency Code** USDOT OST-R
15. Supplementary Notes N/A		

16. Abstract

This project quantifies practical performance indices for signalized corridors using low-resolution data from loop detectors and connected vehicles. Traditionally, such metric quantifications do not sufficiently incorporate considerations for fuel consumption or greenhouse gas emissions. Our approach is to estimate the latent traffic state, i.e., queue length, from the data and then utilize the expressions for performance metrics in terms of queue length to quantify performance. We implement the methodology in PTV VISSIM[7], allowing us to compare our estimates with direct performance metrics. The entire framework is illustrated for two signalized corridors, each with 10 intersections, one in downtown Los Angeles and the other in downtown Long Beach. We compare performance evaluation under fixed time and an adaptive traffic signal policy in these case studies. The percentage difference between fixed-time and adaptive signal control can be used to indicate potential improvement and to rank corridors. This could potentially contribute towards the development of the 2025 State Highway System Management Plan (SHSMP) by Caltrans.

17. Key Words	**18. Distribution Statement** No restrictions.		
19. Security Classif. (of this report) Unclassified	**20. Security Classif. (of this page)** Unclassified	**21. No. of Pages** **19**	**22. Price** N/A

About the Pacific Southwest Region University Transportation Center

The Pacific Southwest Region (PSR) University Transportation Center (UTC) is the Region 9 University Transportation Center funded under the United States Department of Transportation's University Transportation Centers Program. Established in 2016, the Pacific Southwest Region UTC is led by the University of Southern California and includes seven partners: Long Beach State University; University of California, Davis; University of California, Irvine; University of California, Los Angeles; University of Hawaii; Northern Arizona University; and Pima Community College.

The Pacific Southwest Region UTC conducts an integrated, multidisciplinary program of research, education and technology transfer aimed at *improving the mobility of people and goods throughout the region.* Our program is organized around four themes: 1) technology to address transportation problems and improve mobility; 2) improving mobility for vulnerable populations; 3) Improving resilience and protecting the environment; and 4) managing mobility in high growth areas.

California Department of Transportation (CALTRANS) Disclaimer

Contents

1 Introduction

This project quantifies practical performance indices for signalized corridors using low-resolution data from loop detectors and connected vehicles. Traditionally, such metric quantifications do not sufficiently incorporate considerations for fuel consumption or greenhouse gas emissions. Our approach is to estimate the latent traffic state, i.e., queue length, from the data and then utilize the expressions for performance metrics in terms of queue length to quantify performance. We implement the methodology in PTV VISSIM[7], allowing us to compare our estimates with direct performance metrics. The entire framework is illustrated for two signalized corridors, each with 10 intersections, one in downtown Los Angeles and the other in downtown Long Beach. We compare performance evaluation under fixed time and an adaptive traffic signal policy in these case studies. The percentage difference between fixed-time and adaptive signal control can be used to indicate potential improvement and to rank corridors. This could potentially contribute towards the development of the *2025 State Highway System Management Plan* (SHSMP) by Caltrans.

2 Literature Review

Adaptive control of traffic signals is a critical approach to improve traffic flow efficiency and reduce environmental impact. To achieve more accurate signal control, queue length estimation has become a core issue in traffic management research. Traditional methods usually rely on loop detector data. Ban *et al.*[2] determined where to locate detectors at a signalized intersection by analyzing the data of vehicles passing through virtual detectors. Zhan *et al.*[3] established an intersection queue length estimation model based on automated traffic enforcement system data and shockwave theory. Liu *et al.*[5] proposed three models based on shockwave theory for different detector data types to calculate maximum queue length.

There are several limitations to the traditional method based on loop detectors, such as low data resolution. In recent years, the application of connected vehicle (CV) data has provided a new direction for queue length estimation. Wang *et al.*[1] used CV trajectories to estimate unknown traffic states and parameters. By representing queue length as a stochastic process, the model in Wang *et al.*[1] estimates the arrival rate and queue length in real time and can accurately capture the formation and dissipation of queues even at a low penetration rate of CV.

3 Queue Length Estimation Models

This section presents two queue length estimation methods based on the detector-based estimation in [5] and CV-based estimation in [1]. Specifically, the detector-based data model uses the second-by-second detector data to estimate the queue length at the signalized intersection; the CV-based data model uses the trajectory data from CV with known penetration rates and a stochastic queuing model to estimate the queue length distribution.

3.1 Detector-based Queue Length Estimation

3.1.1 Breakpoints Identification

Based on the second-by-second detector occupancy data, three breakpoints need to be identified first.

- **Formation Point T_A^n**

  Let $T_{occupy}(t)$ denote the duration of time the detector has been continuously occupied immediately before and through time t. Let T_A^n denote the time when $T_{occupy} \geq 3$ seconds the first time during the n^{th} traffic signal cycle, indicating that a queue begins to form. Let T_g^n represent the end time of the green phase in the n^{th} cycle. Then, T_A^n can be calculated as follows:

$$T_A^n = \underset{t}{argmin}\{t | T_{occupy}(t) \geq 3, t \in [T_g^n, T_g^{n+1}]\} \quad (3-1)$$

- **Discharge Point T_B^n**

  Let T_B^n denote the time when $T_{occupy} < 3s$ the first time after T_A^n, indicating that the queue begins to dissipate, vehicles begin to

leave the queue. Then, T_B^n can be calculated as follows:

$$T_B^n = argmin_t\{t|T_{occupy}(t) \le 3, t \in [T_A^n, T_g^{n+1}]\} \quad (3-2)$$

- **Clearance Point T_C^n**

  After T_B^n, let T_C^n denote the time when time duration between two vehicles passing the detector is greater than 2.5 seconds, indicating that the formed queue has dissipated, and the queue length is zero.

3.1.2 Shockwave Speed

Let L_d denote the distance between the stop line and the detector; let T_r^n denote the start time of red phase. When vehicles start to queue up at the start of red phase, the speed of the shockwave v_2 propagating backward formed at the head of the queue can be calculated as

$$v_2 = \frac{L_d}{T_B^n - T_r^n} \quad (3-3)$$

When the queue starts to dissipate as the red phase ends and the green phase begins, the forward propagating shockwave velocity v_3 formed at the tail of the queue can be calculated as

$$v_3 = \frac{L_d + (T_C^n - T_B^n)}{T_C^n - T_B^n} \quad (3-4)$$

3.1.3 Maximum Queue Length and Maximum Queuing Time

Let k_j denote jam density. All vehicles passing the detector between T_r^n and T_C^n are considered in the queue. Then, the maximum queuing space L_{max}^n and maximum queuing time T_{max}^n can be calculated as follows:

$$\begin{cases} L_{max}^n = (V^n/k_j) + L_d \\ T_{max}^n = T_r^n + \dfrac{L_{max}^n}{v_2} \end{cases} \quad (3-5)$$

where V^n is the maximum number of vehicles in the queue during the n^{th} signal cycle.

3.2 CV-based Queue Length Estimation

Although detector-based models can effectively estimate the queue length, it requires high data quality. In addition, the model relies on the assumption of fixed detector positions, which makes it difficult to accurately describe the changes at the end of the queue under dynamic traffic conditions. In CV-based estimation, CV trajectories are assumed to be random samples of the entire traffic flow to recover queue length from limited observation data. Since CVs are moving on the traffic network and data can be collected at every location, CV-based method is adaptive to dynamic traffic conditions.

3.2.1 Arrival Rate

CVs are assumed to be a portion of vehicles randomly selected from all vehicles in proportion to the given penetration rate ϕ, and the traffic parameters of these vehicles are extracted, such as speed, location, etc. These selected vehicles are considered observation samples and are used to infer the dynamic behavior of the entire traffic network. Let $N_c(t)$ denote the total number of signal cycles by time t. Using the arrival time of the selected sample vehicles, the arrival rate $a(t)$ at time t can be calculated as

$$a(t) = \frac{n_c(t)}{N_c \cdot \Delta u \cdot \phi} \quad (3-8)$$

where $n_c(t)$ is the total number of CVs that are present in the queue by time t; Δu is the saturation flow rate per time step.

3.2.2 Queue Length

At time t, let $b(t)$ denote the departure rate; and let $x(t,k)$ denote the probability that the queue length is equal to k. The evolution of $x(t,k)$ is given by

$$x(t,k) = x(t-1,k-1) \cdot a(t) + x(t-1,k) \cdot \big(1 - a(t)\big) \quad (3-9)$$

where $x(t-1,k-1)\, a(t)$ represents the probability that a new vehicle arrives at time t (with probability $a(t)$) and the queue length increases from $k-1$ to k; $x(t-1,k)\,(1-a(t))$ represents the probability that no new vehicle arrives at time t (with probability $(1-a(t))$ and the queue length remains k.

The departure rate $b(t)$ can be calculated as

$$b(t) = S(t)\Sigma_{k=1}^{N} x(t,k) \quad (3-10)$$

where N is the maximum queue length; $S(t) \in \{0,1\}$ indicates the traffic signal state, i.e.,

- When $\boldsymbol{S(t) = 1}$, the traffic signal is green, and the vehicle can leave, queue length $\boldsymbol{q(t)}$ is given by

$$q(t) = [max(q(t-1) - b(t), 0)] \cdot \Delta u \quad (3-11)$$

- When $\boldsymbol{S(t) = 0}$, the traffic signal is red, and the vehicle cannot leave, queue length $\boldsymbol{q(t)}$ is given by

$$q(t) = [q(t-1) + a(t) \times \big(1 - \Sigma_{k=1}^{N} x(t-1,k)\big)] \cdot \Delta u \quad (3-12)$$

4 Traffic Signal Adaptive Control Algorithm

This section proposes an adaptive signal control algorithm to improve traffic efficiency. The signal control algorithm maximizes through band in a preferred direction, i.e., north-south direction (main road), across different intersections and adjusts green time duration at each intersection. In this project, the cycle length is set to be $t_{cycle} = 60s$ for simplicity. More complicated method for determining cycle length can be useful and will be pursued in the future.

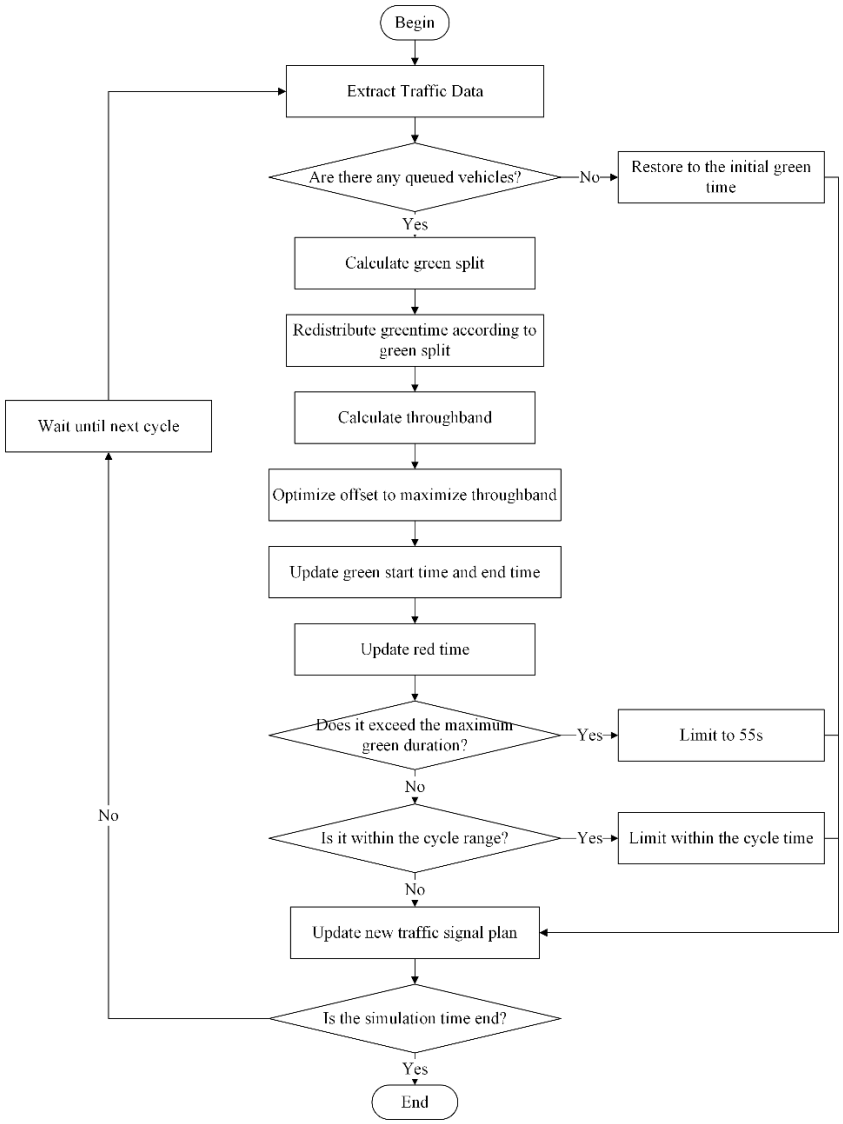

Fig. 4.1 Flowchart of Adaptive Signal Control

4.1 Green Time

In this project, the signal timing design includes two phases: the north-south phase and the east-west phase. The north-south direction is the main road and has a higher priority to ensure the traffic efficiency of the main road. According to the maximum queue length, the green split in the north-south (NS) and east-west (WE) directions is calculated:

$$\alpha_{NS} = \frac{q_{t-NS}}{q_{t-NS} + q_{t-WE}} \tag{4-1}$$

$$\alpha_{WE} = \frac{q_{t-NS}}{q_{t-NS} + q_{t-WE}} \tag{4-2}$$

where q_{t-NS} represents the estimated maximum queue length of all lanes in the NS direction, and q_{t-WE} represents the maximum queue length of all lanes in the WE direction. If queue lengths are zero in both directions, the default allocation is: $\alpha_{NS} = \alpha_{WE} = 0.5$.

Using the cycle time t_{cycle}, the green duration can be calculated as:

$$t_{G-NS} = t_{cycle} \times \alpha_{NS} \tag{4-3}$$

$$t_{G-WE} = t_{cycle} \times \alpha_{WE} \quad (4-4)$$

To prevent the calculated t_G from being too small or too large and exceeding the cycle time, the calculation result is constrained:

$$t'_G = min(max(t_G, t_{G-min}), t_{G-max}) \quad (4-5)$$

where t_{G-min} represents the minimum green duration, t_{G-max} represents the maximum green duration. In this project, $t_{G-min} = 5s$, $t_{G-max} = 55s$.

4.2 Through band

The through band on the entire corridor can be integrated into a continuous green wave by adjusting the offset and optimizing the start and end time of the green signal. As a result, vehicles on the major road can pass through multiple consecutive intersections in sequence while maintaining speed without stopping and waiting for green signal frequently. Let $B^{i,n}$ denote the width of the through band between the i^{th} intersection and the $(\mathrm{i}+1)^{th}$ intersection at cycle n, and let $[T^{i,n}_{G-start}, T^{i,n}_{G-end}]$ and $[T^{i+1,n}_{G-start}, T^{i+1,n}_{G-end}]$ denote green signal periods at i^{th} and $(\mathrm{i}+1)^{th}$ intersections, respectively. The through band $B^{i,n}$ can be calculated as follows:

$$B^{i,n} = \min(T^{i,n}_{G-end}, T^{i+1,n}_{G-end}) - \max(T^{i,n}_{G-start}, T^{i+1,n}_{G-start}), \forall i \in 1, 2, \dots, m-1 \quad (4-6)$$

The length of the optimization cycle can be adjusted at any time. In this paper, it is set to be the same as the signal cycle t_{cycle}, i.e., the traffic signal is optimized every 60s.

Let $O_{i,n}$ represent the offset of the i^{th} intersection at cycle n, and let $O^*_{i,n}$ represent the offset when the through band is the maximum, i.e.,

$$O^*_{i,n} = \underset{O_{i,n}}{\operatorname{argmax}} B^{i,n} \quad (4-7)$$

After obtaining the optimized offset $O^*_{i,n}$, the start time $T^{i,n+1}_{G-start}$ of the green signal in the following $(\mathrm{n}+1)^{th}$ optimization cycle and the corresponding end time $T^{i,n+1}_{G-end}$ can be obtained as follows:

$$T^{i,n}_{G-start} = \left(T^{i,n}_{G-start} + O^*_{i,n}\right) \bmod t_{cycle} \quad (4-8)$$

$$T^{i,n+1}_{G-end} = \left(T^{i,n+1}_{G-start} + t'_G\right) \bmod t_{cycle} \quad (4-9)$$

4.3 Red Time

The traffic signal is set to red at the initial time $t = 0s$ in each signal cycle, and $T^n_{R-end} = t^n_R$. Additionally, the red signal duration needs to satisfy the following constraints and the total cycle time cannot exceed $60s$:

$$t_{R-min} = t_{cycle} - t_{G-max} - t_{Amber} = 3s \quad (4-10)$$

$$t_{R-max} = t_{cycle} - t_{G-min} - t_{Amber} = 53s \quad (4-11)$$

$$t_R{}' = min(max(t_R, t_{R-min}), t_{R-max}) \quad (4-12)$$

where t_{R-min} represents the minimum duration of the red signal, t_{R-max} represents the maximum duration of the red signal, t_{Amber} is the Amber Time and is set to be $t_{Amber} = 2s$.

5 Simulation Setup and Verification of Queue Length Estimation

5.1 Model Setup in VISSIM

This project uses PTV VISSIM to create road networks, following appropriate geometric scales based on Bing Maps. All vehicle types in the network are set to 'Car', and the default speed of vehicles is 40 km/h. For simplicity, pedestrians are not included in the simulation.

In terms of vehicle flow and path decision, the simulation model defines the external arrival rate to represent the flow of vehicles entering

the network from the input point. The external arrival rate is expressed in the number of vehicles per hour and is used to simulate actual traffic demand. For the vehicle path decision of each intersection, the proportion of turning flow is defined by setting the 'RelFlow' parameter. These parameter values are set at the initialization of the simulation and can be adaptively adjusted during the simulation process through the COM interface to adapt to real-time traffic changes and simulation requirements.

The road network sets signal heads at the end of the entrance of lanes for every intersection. The initial signal plan is based on average flow ratios in two directions and implemented in the 'Signal Program' module of VISSIM. In addition, to accurately model the turning path and driving priority of the vehicle, the 'Conflict Area' module is set in the model to reflect the possible conflict and priority rules in the intersection.

To ensure the simulation's rationality, the vehicle's saturation flow rate is set to 1900 veh/hr/lane in this paper, consistent with the standard value recommended by the *Highway Capacity Manual 2000*.

This project selected two traffic corridors as examples to validate the algorithms proposed in Section 3 based on the vehicle dynamic data generated by VISSIM simulation. The examples are Flower Street in downtown Los Angeles (DTLA), as shown in *Fig. 5.1 (1)*, and Atlantic Avenue in Long Beach, as shown in *Fig. 5.1 (2)*. Both corridors contain 10 intersections with traffic signals.

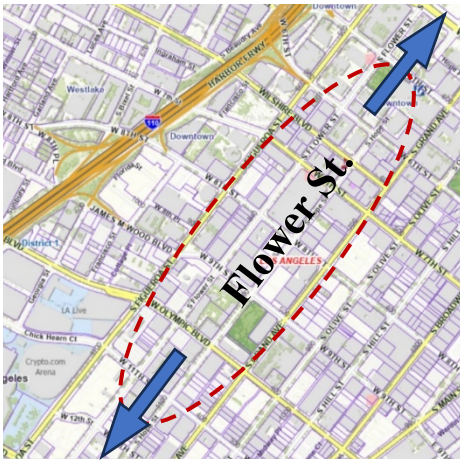

Fig. 5.1 (1) Traffic Corridor in DTLA

Fig. 5.1 (5.1) Traffic Corridor in Long Beach

Before adaptively allocating the signal duration, it is necessary to first verify the accuracy of the two queue length algorithms by comparing and analyzing the simulation results. The actual queue length generated by the VISSIM simulation model is used as the benchmark value (simulated value), and the estimated values obtained by the two algorithms are compared with the simulated values. This report takes the traffic corridor consisting of ten consecutive intersections on Flower Street in DTLA as the testbed to evaluate the applicability of the two queue length estimation algorithms under different traffic flow conditions.

5.2 Verification of Estimation Methods

At every simulation time step, vehicle locations and vehicle speed are extracted to calculate the exact queue length. We count all vehicles such that speed is less than 5 mph and headway between adjacent vehicles is less than 32 ft in queue length calculation. Then, we compare the exact queue length and estimated queue lengths using detector and CV-based methods described in Section 3.2.

5.2.1 Verification of Detector-based Method

We first evaluate the estimation accuracy of detector-based method. We install detectors at the entry link in Flower St. where large queues are present. Three detectors are used indexed by No. 70, 71, and 72. The indices are chosen based on their relative distance to the stop line of the intersection and the middle of the link. In other words, detector No. 70 is located near the stop line; detector No. 71 is located between the stop line and the middle of the link, and detector No. 72 is located in the middle of the link. Fig. 5.2 shows the mean absolute percentage errors (MAPE) between the estimated queue lengths from the model and exact queue lengths from VISSIM under different traffic volume scenarios. It can be concluded that the detector-based method is more accurate when traffic volume is medium.

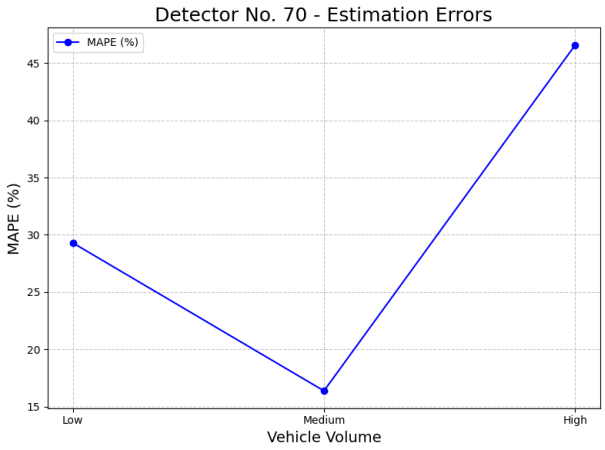

Fig. 5.2 (1) Estimation errors by using Detector No. 70

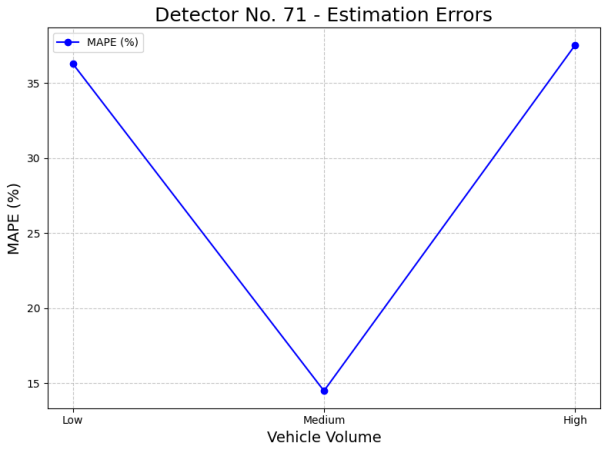

Fig. 5.2 (2) Estimation errors by using Detector No. 71

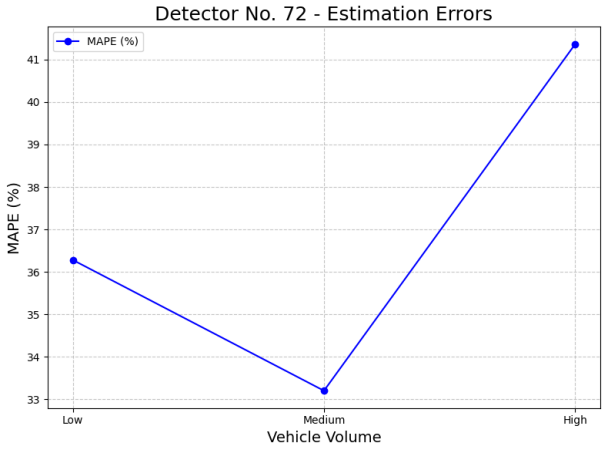

Fig. 5.2 (3) Estimation errors by using Detector No. 72

Fig. 5.3 further explores the effect of the number of cycles on the estimation error using detector 71 in medium traffic. As the number of cycles increases, the estimation errors first decrease but then increase to around 15%.

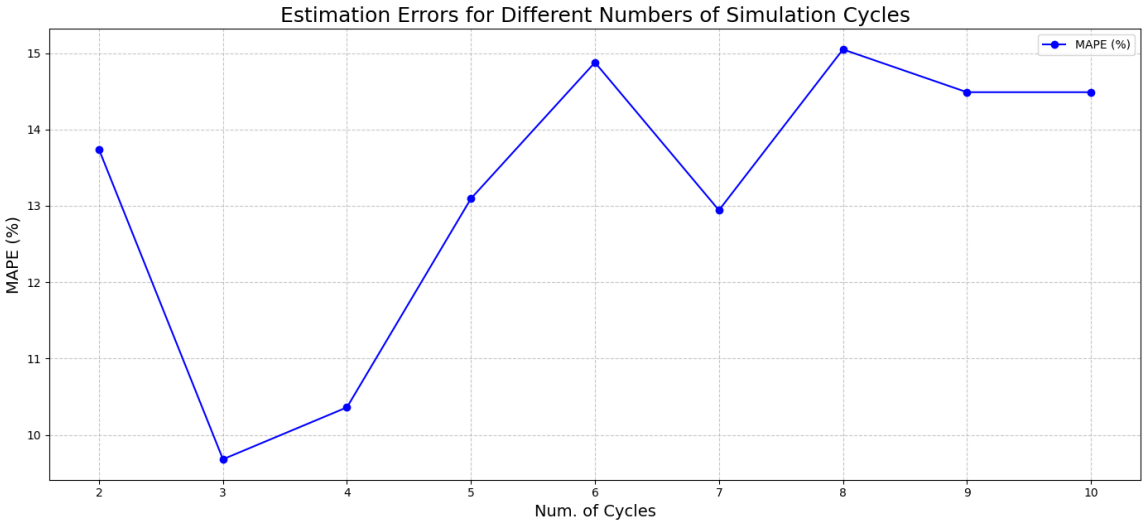

Fig. 5.3 Estimation errors for different numbers of simulation cycles

This trend shows that the choice of the number of cycles is critical to the accuracy and stability of queue length estimation. A smaller number of cycles may lead to insufficient capture of the traffic status. When the number of cycles gradually increases, the error tends to

be stable.

5.2.2 Verification of CV-based Method

Then, we evaluate the estimation errors for CV-based estimation. As shown in Fig. 5.4, for the same traffic volume, the larger the value of ϕ, the smaller the error between the estimated data and the simulated data; when the value of ϕ is the same, the larger the traffic volume, the smaller the error between the estimated data and the simulated data. This is because the penetration rate ϕ represents the proportion of CV vehicles on the road. When the number of CV vehicles increases, information can be collected and transmitted more accurately, improving the estimation accuracy of the queue length, thereby reducing the percentage error.

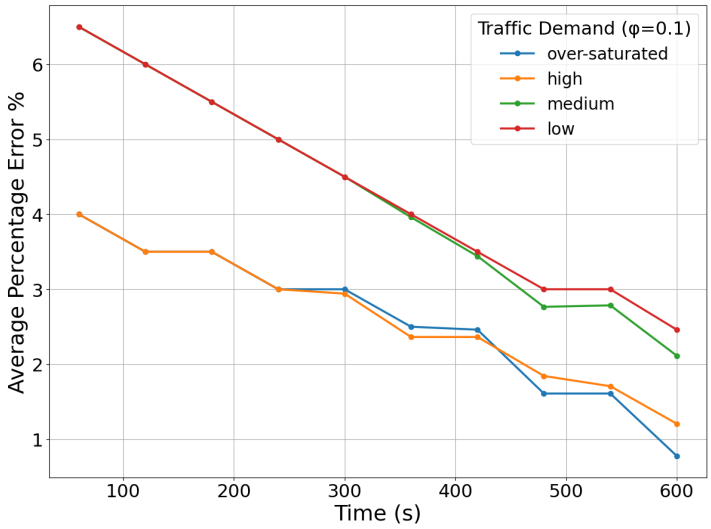

Fig. 5.4(1) Average percentage error for different volume

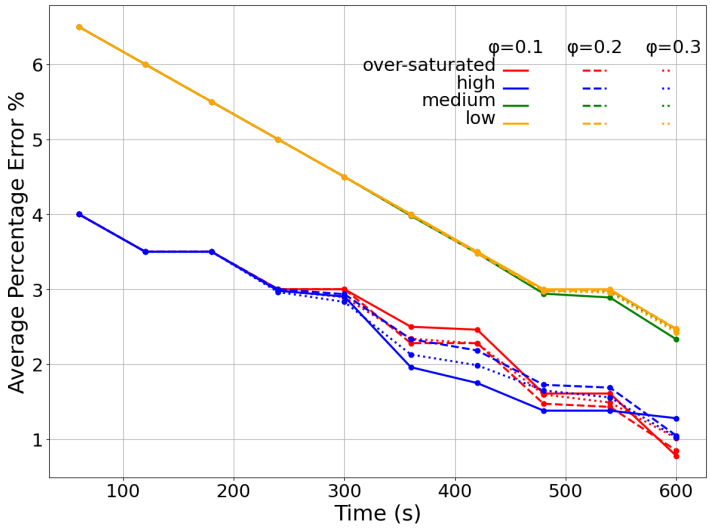

Fig. 5.4(2) Average percentage error for different ϕ

By comparing the errors between the detector and CV-based estimation, the algorithm based on CV data showed higher accuracy in all traffic flow states (including low flow, medium flow, high flow, and supersaturated flow), and the overall error was significantly smaller than another algorithm. In addition, the algorithm's performance is particularly outstanding at low penetration rates, and the error gradually decreases over time, indicating that the algorithm can further improve the estimation accuracy. Based on the verification result, this project selects the CV-based queue length for adaptive signal timing optimization.

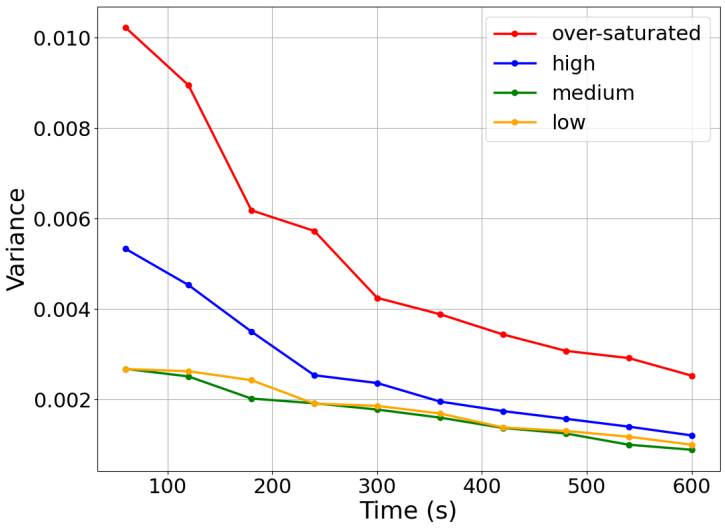

Fig. 5.5(1) Variance of errors for different volume

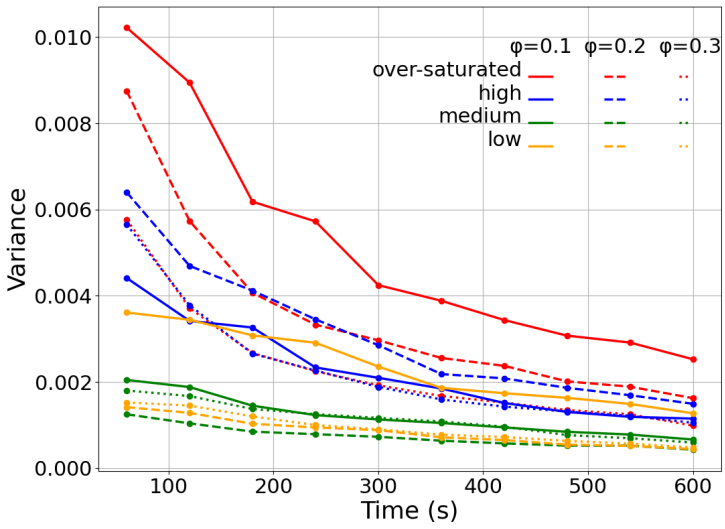

Fig. 5.5(2) Variance of errors for different ϕ

6 Emission models

In this section, we develop models that convert traffic states into emission performance. The internal emission metric in VISSIM and

the basic version of the EPA MOVES model are used as references for the emission model.

VISSIM uses the functions in the external emission model called EmissionModel.dll file to calculate and output the quantities of various pollutants for every link segment. This model can be implemented and activated for diverse vehicle types, including cars, heavy goods vehicles (HGV), buses, and trams, depending on the traffic composition of the VISSIM network.

EPA MOVES is a modeling software that can estimate vehicle emissions with traffic states as input. In this project, traffic data from VISSIM simulations are used as input into EPA MOVES. Key parameters, including location, time, link types, and vehicle types, are extracted from the settings of the VISSIM network. Other input data, such as age distribution of vehicles, fuel information, and meteorology data, are sourced from default databases provided by MOVES4.0. These default data represent the national average or information from the U.S. Environmental Protection Agency (EPA).

Following Han *et al.*[3] and references therein, the relationship between emission and traffic volumes for a given link can be described as a linear function. Here, we aim to reconstruct the model using linear regression. We first examine the emission data from VISSIM. In VISSIM, the first 600 seconds of the simulation are excluded from the analysis to ensure steady traffic flow. Since the default EmissionModel.dll in VISSIM returns constant emission values for each vehicle at every timestep, the relationship between the volume of vehicles (in units of number of vehicles over 3000 seconds) and VISSIM-estimated emission quantities (in units of grams over 3000 seconds) is investigated. The results of the regression model for VISSIM data are presented in *Eq. 4-11a – Eq. 4-11d*:

$$\boldsymbol{Emission\ of\ CO} = 0.02 \times Volume + 4.440, \quad R^2 = 1.0 \qquad (6-1a)$$

$$\boldsymbol{Emission\ of\ NO_x} = 0.08 \times Volume + 1.776, \quad R^2 = 1.0 \qquad (6-1b)$$

$$\boldsymbol{Emission\ of\ PM2.5} = 0.26 \times Volume + 7.105, \quad R^2 = 1.0 \qquad (6-1c)$$

$$\boldsymbol{Aggregated\ emissions\ of\ 3\ pollutants} = 0.36 \times Volume, \quad R^2 = 1.0 \qquad (6-1d)$$

We conjecture that VISSIM also uses linear function of volumes to calculate emission since the R-square values of different emission models are all equal to one.

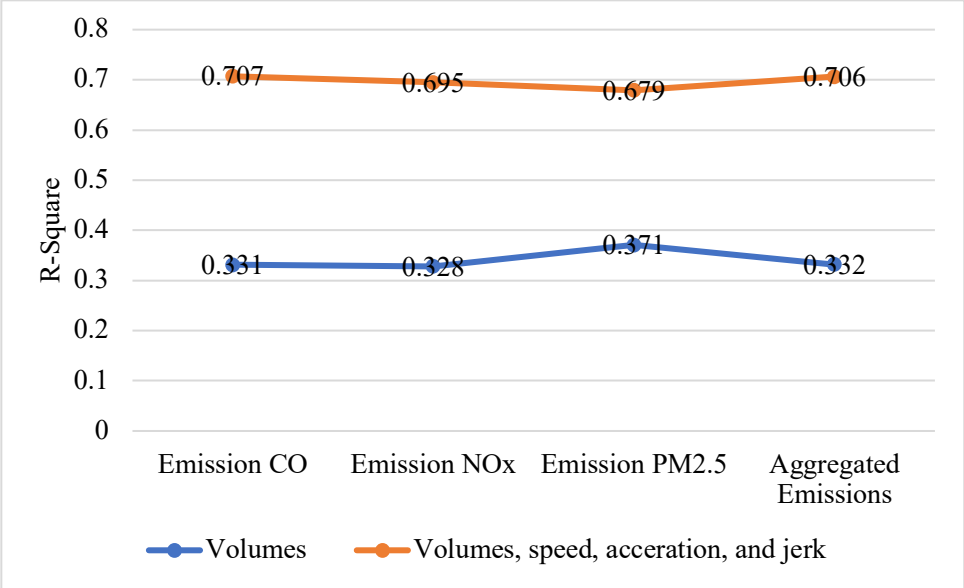

Fig. 6.1 R^2 of linear regressions for MOVES emission data

Then, we run linear regression for emission data generated by EPA MOVES. The regression is conducted using one hour of traffic data. As shown in Fig. 6.1, the R-square values are only around 0.3 when traffic volume is included in linear regression. This suggests that MOVES emission data are not linear in terms of traffic volumes. Then, we incorporate more traffic states into the linear regression model to investigate the linear relationship. Four traffic states are selected: vehicle volume (vehs/h), speed (mph), acceleration (ft/s^2),

and jerk (the rate of change of acceleration (ft/s^3)). After incorporating more traffic states into linear regression, the R-square values improve to nearly 0.7. The final expressions are given as follows:

$$\boldsymbol{Emission\ of\ CO} = 0.04096 \times Volume + 0.01051 \times Speed + 0.11117 \times Acceleration + 0.06639 \times Jerk + 0.0082 \quad (6-2a)$$

$$(R^2 \approx 0.7068)$$

$$\boldsymbol{Emission\ of\ NO_x} = 0.00127 \times Volume + 0.00036 \times Speed + 0.00381 \times Acceleration + 0.00127 \times Jerk + 0.00032 \quad (6-2b)$$

$$(R^2 \approx 0.6945)$$

$$\boldsymbol{Emission\ of\ PM2.5} = 2.6024 \times 10^{-5} \times Volume + 9.2649 \times 10^{-6} \times Speed + 5.8393 \times 10^{-5} \times Acceleration + 2.0205 \times 10^{-5} \times Jerk + 8.4945 \times 10^{-6}$$

$$(R^2 \approx 0.6793) \quad (6-2c)$$

$$\boldsymbol{Aggregated\ emissions\ of\ 3\ pollutants} = 0.04235 \times Volume + 0.01073 \times Speed + 0.12099 \times Acceleration + 0.06431 \times Jerk + 0.00866 \quad (6-2d)$$

$$(R^2 \approx 0.7058)$$

7 Performance evaluation

In this section, we compare the performance before and after implementing the signal control algorithm described in Section 4 on both DTLA and Long Beach corridors. The performance metrics include throughput and emission. The emission model is the one described in Section 6, and the throughput calculation is introduced in the following section.

7.1 Throughput analysis

The throughput of a network is determined by traffic demand, i.e., the external inflow rate that enters the network. In VISSIM simulations, vehicles that cannot enter the network due to congestion in the entry link will be dropped. We use drop rate to represent the percentage of dropped vehicles among all traffic demand. Given a demand profile, the network throughput is equal to the inflow rate if the drop rate is less than certain thresholds. In this project, we evaluate the throughput performance of the two corridors in VISSIM by calculating the drop rate under different traffic demands. To investigate the sensitivity of throughput against different drop rate thresholds, we compare throughputs using 1%, 3%, and 5% as drop rate thresholds.

For DTLA corridor, *Fig. 7.1 (1)* illustrates the relationship between throughput and penetration rate ϕ. When ϕ equals 0, the original traffic signal plan is used as described in section 5.1. When the penetration rate increases from 0 to 0.1, the throughput increases significantly, indicating that even a low penetration rate has a significant positive effect on traffic efficiency. However, when the penetration rate exceeds 0.1, the improvement rate of throughput significantly slows down, meaning that the marginal benefit of ϕ decreases. Further increasing the penetration rate will have a very limited improvement in throughput. Similarly, *Fig. 7.1 (2)* shows the relationship between throughput and penetration rate ϕ of the Long Beach corridor with the same trend as the DTLA corridor.

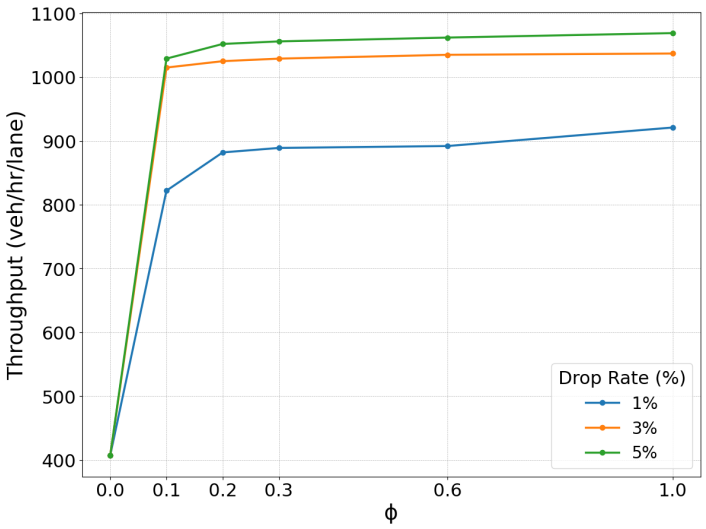

Fig. 7.1 (1) Throughput vs. ϕ with different drop rates in DTLA

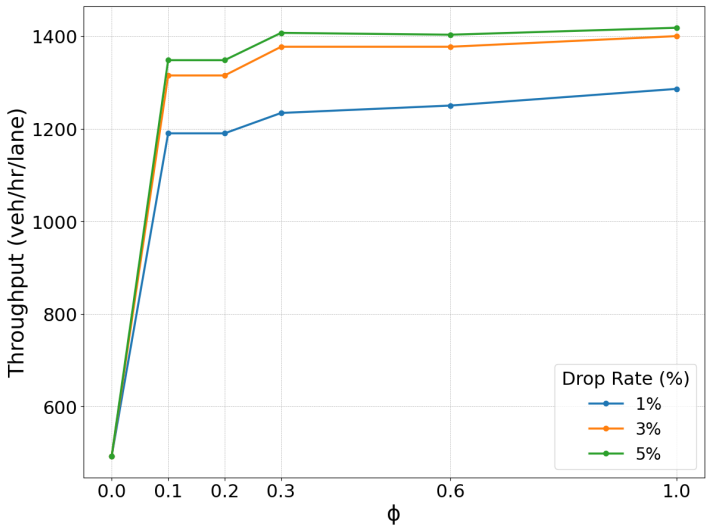

Fig. 7.1 (2) Throughput vs. ϕ with different drop rates in Long Beach

7.2 Emission analysis

In addition to throughput, we evaluate emission performance in VISSIM based on methods introduced in Section 6. Fig. 7.3 (1) shows emission reduction rate calculated in low, medium, and high traffic demand scenarios using VISSIM-based emission model. It can be seen that the signal control algorithm is able to reduce emissions by more than 10%. However, the MOVES-based emission model shows that emissions increase after implementing the signal control for all three traffic demand scenarios, as shown in *Fig. 7.3 (2)*. The inconsistency might be because the VISSIM-based emission model is mainly determined by traffic volumes whereas the MOVES-based emission model is more complicated and considers other factors, such as speed, acceleration, and jerk into emission calculation.

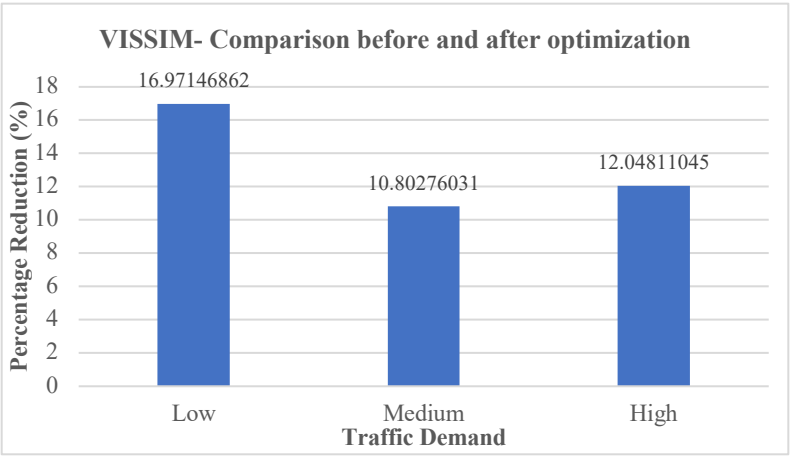

Fig. 7.3 (1) Emission comparison from VISSIM before and after signal optimization in DTLA

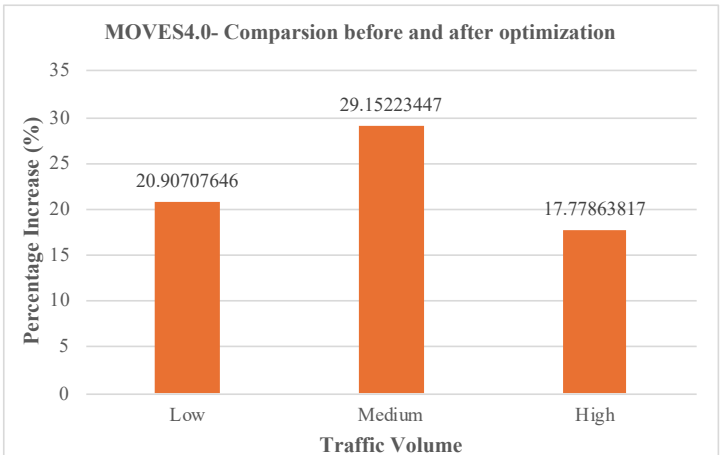

Fig. 7.3 (2) Emission comparison from MOVES before and after signal optimization in DTLA

Fig. 7.4 shows emission results for the Long Beach corridor under different penetration rates ϕ with high traffic demand. When ϕ equals 0, the initial traffic signal plan is used as described in section 5.1. Unlike the DTLA corridor, both VISSIM and MOVES-based emission models suggest that emissions increase after the implementation of the signal control algorithm.

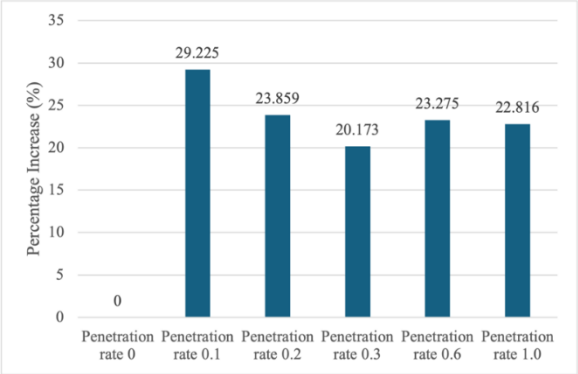

Fig. 7.4 (1) Emission comparison from VISSIM before and after signal optimization in Long Beach

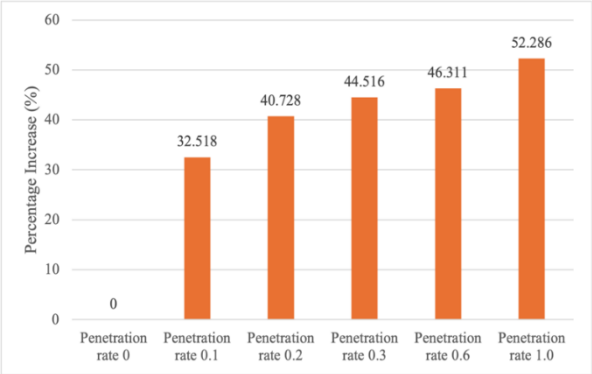

Fig. 7.4 (2) Emission comparison from VISSIM before and after signal optimization in Long Beach

7.3 Performance Comparison of Two Corridors

The performance before and after optimizing traffic signal timing is summarized in *Table 7-1*. We consider the case where the demand is high, and the penetration rate of the connected vehicles is equal to 0.1. The throughput is increased significantly for both corridors. However, emissions calculated from EPA MOVES are also increased. The results suggest a tradeoff between throughput improvement and emission reduction.

Table 7-1 Performance difference before and after optimizing signal timing

Performance/ Corridors	**Flower St.**	**Atlantic Ave.**
Throughput difference	+162%	+185%
VISSIM Emission difference	-12%	+18%
MOVES Emission difference	+18%	+33%

8 Conclusion

In this project, we implemented detector-based and CV-based queue length estimation methods and combined them with signal control algorithms in PTV VISSIM. The goal is to evaluate the performance improvement on two corridors in downtown Los Angeles and Long Beach. The CV-based estimation shows superior accuracy and adaptability across varying traffic demand scenarios. Notably, under lower penetration rates, the estimation error decreases significantly. This highlights its robustness to inaccuracies in sample data, as it compensates for data limitations through probabilistic inference, maintaining reliable estimation even under low-precision conditions. In comparison, detector-based estimation exhibits relatively lower accuracy and adaptability despite efforts to reduce errors by optimizing detector placement. The primary limitation lies in their dependence on fixed detector locations, which restricts their capacity to adapt to dynamic traffic flow changes. Consequently, the CV-based model offers notable advantages in estimation performance over its detector-based counterpart.

The performance metrics in this project consist of throughput and emission. For efficient emission computation, we developed linear models to represent emissions by traffic state data that are more accessible in practice. We also showed that including speed, acceleration, and jerk as regression variables can further improve EPA MOVES-based model accuracy compared to literature where only traffic volume is typically used in linear models.

The signal control algorithm was shown to improve throughput performance significantly. However, this improvement could come with an environmental trade-off, as emissions increased in our simulations based on EPA MOVES calculations. This phenomenon has also been observed in previous studies, e.g., see [10]. These findings suggest that while optimizing traffic efficiency effectively increases corridor capacity, it may also intensify environmental impacts. Further analysis needs to be conducted to investigate the reason behind improved throughput and increased emissions.

Acknowledgment

The project work and report were executed in collaboration with Xinyi Wu, Zhexian Li and Zixiong Zhang, all with the University of the Southern California.

Disclosure

K. Savla has financial interest in Xtelligent, Inc.

Reference

[1] Wang, X. *et al.* Traffic Light Optimization with Low Penetration Rate Vehicle Trajectory Data. *Nature Communications*, 2024, 15(2).

[2] Ban, X. *et al*. Real Time Queue Length Estimation for Signalized Intersections Using Travel Times from Mobile Sensors. *Transportation Research Part C*, 2011(19), 1133-1156.

[3] Zhan, X. *et al.* Lane-Based Real-Time Queue Length Estimation Using License Plate Recognition Data. *Transportation Research Part C: Emerging Technologies*, 2015, 57, 85-102.

[4] Tao, K. *et al*. Study on the Estimation Method of Queue Length at Signalized Intersection. China Public Security, 2015(2), 64-67.

[5] Liu, H. *et al*. Real-time Queue Length Estimation for Congested Signalized Intersections. *Transportation research part C: emerging technologies*, 2009, 17(2).

[6] Pouyan, H. and K. Savla. A comparison study between proportionally fair and max pressure controllers for signalized arterial networks. Transportation Research Board 95th Annual Meeting, No. 16-6738. 2016.

[7] PTV Vissim 2024 MANUAL, 2023. Karlsruhe, Germany: PTV Planung Transport Verkehr GmbH.

[8] U.S. Environmental Protection Agency. Motor Vehicle Emission Simulator (MOVES). https://www.epa.gov/moves.

[9] Han, K. *et al*. "A robust optimization approach for dynamic traffic signal control with emission considerations." *Transportation Research Part C: Emerging Technologies* 70 (2016): 3-26.

[10] Stevanovic, A. *et al*. "Multi-criteria optimization of traffic signals: Mobility, safety, and environment." Transportation Research Part C: Emerging Technologies 55 (2015): 46-68.

Appendix

[1] Pseudocode of Section 3.1 for queue length estimation and shockwave speed calculation

1: **Algorithm 1**: Queue Length Estimation and Shockwave Speed Calculation
2: **Input**: second-by-second detector occupancy data from VISSIM
3: **Output**: $T_A, T_B, T_C, v_2, v_3, v_2, L_{max}^n, T_{max}^n$
4: **MAIN**:
5: **READ** second-by-second detector occupancy data
6: **IDENTIFY** Breakpoints:
7: **FOR** time after effectiveGreenEndTime(n) && before effectiveGreenEndTime(n+1)
8: **IF** detectorOccupancyTime > 3s THEN
9: **CALCULATE** T_A ← Equation (3-1)
10: **ELSE**
11: **CONTINUE**
12: **ENDIF**
13: **ENDFOR**
14: **FOR** time after T_A && before effectiveGreenEndTime(n+1)
15: **IF** detectorOccupancyTime < 3s THEN
16: **CALCULATE** T_B ← Equation (3-2)
17: **ENDIF**
18: **ENDFOR**
19: **FOR** time after T_B && before effectiveGreenEndTime(n+1)
20: **IF** timeGap > 2.5s THEN
21: **CALCULATE** T_C ← Equation (3-3)
22: **ELSE**
23: **PRINT** "Oversaturation"
24: **ENDIF**
25: **ENDFOR**
26:
27: **FUNCTION** calculateShockwaveVelocity($T_A, T_B, T_C,\ L_d,\ T_r^n$):
28: **CALCULATE** v_2 **RETURNING** v_2 ← Equation (3-4)
29: **CALCULATE** v_3 **RETURNING** v_3 ← Equation (3-5)
30:
31: **FUNCTION** calculateMaximum Queue Length and Maximum Queuing Time(data, $T_r^n,\ k_j$)
32: **CALCULATE** Maximum Queue Length and Queuing Time:
33: **CALCULATE** L_{max}^n **RETURNING** L_{max}^n ← Equation (3-6)
34: **CALCULATE** T_{max}^n **RETURNING** T_{max}^n ← Equation (3-7)

[2] Pseudocode of Section 3.2 for arrival rate and queue length estimation

1: **Algorithm 2**: Arrival Rate and Queue Length Estimation
2: **Input**: Selected sample vehicles data, $t_{cycle},\ \phi$
3: **Output**: $a(t),\ q(t)$
4: **MAIN**:

5: **FUNCTION** calculateArrivalRate($t_{cycle}, n(\mathrm{t}), \Delta u, \phi$)
6: **CALCULATE** Arrival Rate:
7: **SET** $N_c = \left\lfloor \frac{\max(\mathrm{t})}{t_{cycle}} \right\rfloor + 1$ ← Equation (3-7)
8: **SET** $a(t) = \frac{n(\mathrm{t})}{N_c \cdot \Delta u \cdot \phi}$ RETURN $a(t)$ ← Equation (3-8)
9: **FUNCTION** updateQueueProbability($x(t-1,k-1), x(t-1,k), a(t)$)
10: **SET** $x'(t,k) = x(t-1,k-1) \cdot a(t) + x(t-1,k) \cdot \big(1 - a(t)\big)$ RETURN $x'(t,k)$ ← Equation (3-9)
11: **FUNCTION** calculateQueueLength($a(t), S(t), x(t,k), q(t-1)$)
12: **CALCULATE** Queue Length:
13: **IF** $S(t) = 1$ THEN ▷ Traffic signal is green
14: **CALCULATE** $b(t) = S(t)\Sigma_{k=1}^{N}\mathrm{x}(t,k)$ ← Equation (3-10)
15: **SET** $q(t) = \max\left(q(t-1) - b(t), 0\right)$ ← Equation (3-11)
16: **ELSE** ▷ Traffic signal is red
17: **SET** $q(t) = q(t-1) + a(t) \times \big(1 - \Sigma_{k=1}^{N} x(t-1,k)\big)$ ← Equation (3-12)
18: **ENDIF**
19: **RETURN** $q(t)$

[3] Pseudocode of Section 4 for adaptive signal control

1: **Algorithm 3**: Adaptive Signal Control
2: **Input**: $t_{cycle}, T_{G-start}^{i}, T_{G-end}^{i}, q_{t-NS}, q_{t-WE}, t_{G-max}, t_{G-min}, t_{Amber}$
3: **Output**: ${T_{G-start}^{i}}', {T_{G-end}^{i}}', t'_{G-NS}, t'_{G-WE}, t'_{R}$
4: **MAIN**:
5: **SET** cycle time $t_{cycle} = 60s$
6: **SET** minimum and maximum green time:
7: $t_{G-min} = 5s$
8: $t_{G-max} = 55s$
9: **SET** amber time:
10: $t_{Amber} = 2s$
11:
12: **CALCULATE** Green Split:
13: **IF** $q_{t-NS} = 0$ **AND** $q_{t-WE} = 0$ **THEN**
14: **SET** $\alpha_{NS} = 0.5$
15: **SET** $\alpha_{WE} = 0.5$
16: **ELSE**
17: $\alpha_{NS} = \frac{q_{t-NS}}{q_{t-NS} + q_{t-WE}}$ ← Equation (4-1)
18: $\alpha_{WE} = \frac{q_{t-NS}}{q_{t-NS} + q_{t-WE}}$ ← Equation (4-2)
19: **ENDIF**
20:
21: **CALCULATE** Green Time:
22: $t_{G-NS} = t_{cycle} \times \alpha_{NS}$ ← Equation (4-3)

$t_{G-WE} = t_{cycle} \times \alpha_{WE}$ ← Equation (4-4)

CONSTRAIN t_{G-NS} **AND** t_{G-WE}:

$t'_{G-NS} = min(max(t_{G-NS}, t_{G-min}), t_{G-max})$ ← Equation (4-5)

$t'_{G-WE} = min(max(t_{G-WE}, t_{G-min}), t_{G-max})$ ← Equation (4-5)

FOR each intersection from 1 to $m-1$ **DO**

CALCULATE width of the through band $B^{i,n}$:

$B^{i,n} = \min(T^{i,n}_{G-end}, T^{i+1,n}_{G-end}) - \max(T^{i,n}_{G-start}, T^{i+1,n}_{G-start})$ ← Equation (4-6)

ENDFOR

OPTIMIZE Through Band Width:

MAXIMIZE total throughband B by optimizing offsets $O^{i,n}$ for all intersections:

$O^{*}_{i,n} = \underset{O_{i,n}}{\operatorname{argmax}} B^{i,n}$ ← Equation (4-7)

UPDATE Signal Timing for Next Optimization Cycle:

FOR each intersection from 1 to $m-1$ **DO**

CALCULATE adjusted green start time:

$T^{i,n}_{G-start} = \left(T^{i,n}_{G-start} + O^{i,n}\right) mod\ t_{cycle}$ ← Equation (4-8)

CALCULATE adjusted green end time:

$T^{i,n+1}_{G-end} = \left(T^{i,n+1}_{G-start} + t'_G\right) mod\ t_{cycle}$ ← Equation (4-9)

ENDFOR

CALCULATE minimum and maximum red signal duration:

$t_{R-min} = t_{cycle} - t_{G-max} - t_{Amber}$ ← Equation (4-11)

$t_{R-max} = t_{cycle} - t_{G-min} - t_{Amber}$ ← Equation (4-12)

FOR each cycle n **DO**

CALCULATE raw red signal duration t^n_R:

$t^n_R = t_{cycle} - t^{n'}_G - t_{Amber}$

CONSTRAIN red signal duration $t^{n\prime}_R$:

$t_R{}' = min(max(t_R, t_{R-min}), t_{R-max})$ ← Equation (4-13)

ENDFOR